Mo_6Se_8-cluster-based superconducting compounds $Cs_2Mo_{12}Se_{14}$ and $Rb_4Mo_{18}Se_{20}$: Evidence for a strongly correlated and anisotropic electron system

R. Brusetti, O. Laborde, and A. Sulpice
Centre de Recherches sur les Très Basses Températures, laboratoire associé à l'Université Joseph Fourier, CNRS, Boîte Postale 166, 38042 Grenoble-Cédex 9, France

R. Calemczuk
Laboratoire de Cryophysique, Centre d'Etudes Nucléaires de Grenoble, Boîte Postale 85 X, 38042 Grenoble-Cédex, France

M. Potel and P. Gougeon
Laboratoire de Chimie Minérale B, Université de Rennes, Avenue du Général Leclerc, 35042 Rennes-Cédex, France

(Received 30 December 1994; revised manuscript received 21 April 1995)

We studied the normal and superconducting states of the title compounds by measuring the conductivity and magnetization of single crystals and powder samples. From the upper and lower critical fields we deduced the characteristic lengths and thermodynamical fields. These results are borne out by our specific-heat measurements. We recognize in these compounds many features of the Chevrel-phase superconductors, including very small coherence lengths and strong-coupling-like effects. However, we show that the electron system is much more anisotropic and still less delocalized in these materials where the Mo_6Se_8 clusters have condensed in $Mo_{6n}Se_{6n+2}$ finite chains. This condensation is accompanied by an enhancement of the magnetic response whereas the lengthening of the chains leads to a counteracting reduction of the density of carriers. This indicates that superconductivity is built upon highly correlated molecular states. Reviewing the available data on the other Chevrel-cluster-based superconductors confirms this picture and suggests that the small coherence lengths reflect the local character of the electron pairing. This comparison also shows that forming finite chains of Mo_6Se_8 clusters makes the electron correlations more repulsive and pushes the electron system near the borderline between superconductivity and magnetism. In this respect these compounds could provide valuable complementary information on issues which are at the center of the research upon high-T_c superconductivity.

I. INTRODUCTION

The debate about the origin of the electron coupling in the high-T_c cuprates is often sustained by comparisons with other superconductors and several attempts have been made to identify the real specificity of the former system, i.e., to establish whether it necessitates a completely novel approach or not. Some supporters of the first point of view recognize that certain superconductors which have fallen out of fashion could also be a matter for the new models: the $A15$, the Chevrel phase, and even the heavy-fermion compounds have been reconsidered in this new light.[1]

We present in this paper the very peculiar properties of two compounds which are able to stimulate this debate. $Cs_2Mo_{12}Se_{14}$ and $Rb_4Mo_{18}Se_{20}$ belong to the $M_{2n-2}Mo_{6n}Se_{6n+2}$ family, standing halfway between two apparently very different superconducting systems: the quasi-isotropic ($n = 1$) Chevrel phase superconductors (CPS)—which have a high electronic density of states at the Fermi level $\mathcal{D}_{E_F}$— and the quasi-one-dimensional ($n = \infty$) $Tl_2Mo_6Se_6$—which has a very low $\mathcal{D}_{E_F}$ but a transition temperature T_c of the same order. The title compounds become superconducting below $T_c \approx 4.5$ K. They result from the condensation of the Mo_6Se_8 clusters along the ternary axis. This process, which finally leads to the infinite chains $(Mo_3Se_3)_\infty$, is schematized in Fig. 1. The preparation of the finite-chain compounds and their crystal structures have been described previously.[2,3]

Our paper is organized as follows: in Sec. II we present the normal-state resistivity and susceptibility of the finite-chain compounds; in Sec. III the low-temperature specific-heat of $Cs_2Mo_{12}Se_{14}$ is described and discussed within the framework of the current models. Section IV is devoted to the measurements of the higher (Sec. IV A) and lower (Sec. IV B) critical fields, from which are derived in Sec. V the thermodynamical fields and the characteristic lengths of the superconducting state. Finally we conclude this paper by discussing the whole set of our data and by comparing the finite-chain compounds to their neighbors in the $M_{2n-2}Mo_{6n}Se_{6n+2}$ family. This brings to the fore convergent clues that the carriers involved in the superconducting condensation are coming from states which are tightly bound to the clusters and

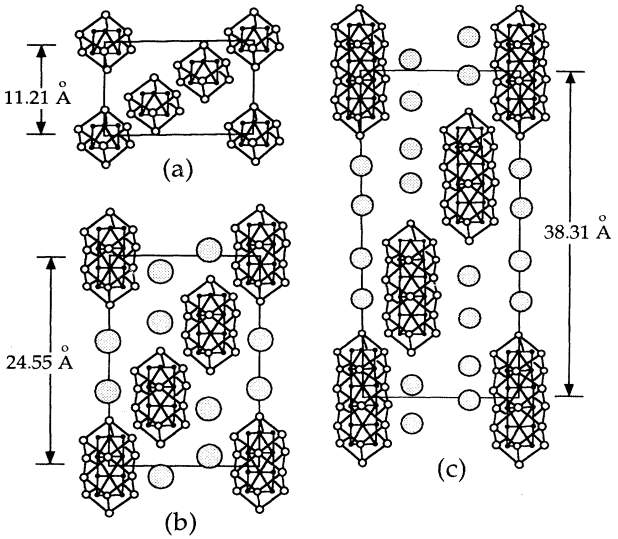

FIG. 1. Projection of the crystal structure of Mo_6Se_8 (a), $Cs_2Mo_{12}Se_{14}$ (b), and $Rb_4Mo_{18}Se_{20}$ (c) onto the $(11\bar{2}0)$ hexagonal plane (Mo: dots; Se: small empty circles; alkali metals: large circles).

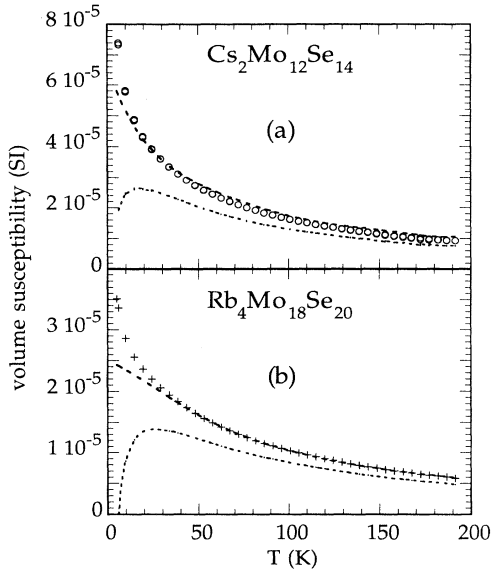

FIG. 3. Magnetic susceptibility of the powder samples of $Cs_2Mo_{12}Se_{14}$ (a) and $Rb_4Mo_{18}Se_{20}$ (b). The points correspond to the low-field measurements (B = 10 mT and 100 mT); the dashed curves have been obtained with $B = 5$ T (data points have been omitted for clarity). The dotted curves are deduced from the previous data after subtraction of a Curie contribution attributed to $S = 5/2$ impurities (see text).

ready to form localized moments. This should allow the $M_{2n-2}Mo_{6n}Se_{6n+2}$ family to serve as a testing ground for the different theoretical treatments of the electron-electron coupling in rather localized electron systems.

II. RESISTIVITY AND SUSCEPTIBILITY IN THE NORMAL STATE

The resistivities along the c axis of single crystals of $Cs_2Mo_{12}Se_{14}$ and $Rb_4Mo_{18}Se_{20}$ have been measured previously[2,3] between 300 K and 4.2 K; we have collected these results in Fig. 2.

Although these crystals have approximately the same large room-temperature resistivity[4] ($\approx$ 6 mΩ cm), they display markedly different behaviors at lower temperature: $Cs_2Mo_{12}Se_{14}$ looks like a semimetal down to $\sim$ 100 K, then it becomes metallic and its resistivity decreases quite linearly between 50 K and $T_c \approx 4.6$ K where it is still $\approx$ 2.6 mΩ cm. The behavior of $Rb_4Mo_{18}Se_{20}$ looks metallic in the whole temperature range with a linear approach to $T_c \approx 4.4$ K where $\rho_{T_c} \approx 500$ $\mu\Omega$ cm; however, above 100 K it clearly tends towards saturation.

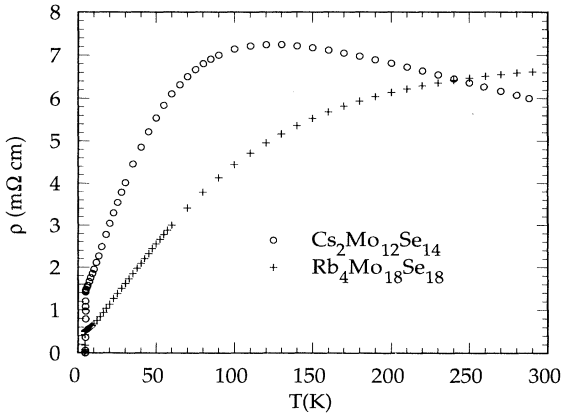

FIG. 2. Resistivity along the ternary (c) axis of $Cs_2Mo_{12}Se_{14}$ (circles) and $Rb_4Mo_{18}Se_{20}$ (crosses) (from Refs. 2 and 3).

The magnetic susceptibility of powder samples have been measured between 2 K and 300 K with a commercial superconducting quantum interference device (SQUID) magnetometer. No parasitic phase can be detected in the x-ray pattern of these samples which have about the same T_c as the corresponding single crystals. Magnetic fields ranging between 10 mT and 5 T have been applied and this revealed a significant nonlinearity of the magnetization curves below about 20 K (see Fig. 3). The temperature dependence of the low-field susceptibility can be fitted quite well by a Curie-Weiss law: $\chi = N\mu_{\text{eff}}^2/3k_B(T-\theta)$. By taking N corresponding to one moment per $M_{2n-2}Mo_{6n}Se_{6n+2}$ molecule we obtain an effective moment $\mu_{\text{eff}} \approx 0.7\ \mu_B$ in both compounds whereas θ would be ≈ -25 K and -38 K in the cesium ($n = 2$) and rubidium ($n = 3$) compounds, respectively. These results are rather surprising and call for some comments. The susceptibility of the CPS often displays an unusually large temperature dependence;[5,6] one possible

interpretation of this phenomenon is that a sharp peak exists in the electron density of states $\mathcal{D}_{E_F}$ and that the Fermi level intersects this peak—which yields a Pauli temperature-dependent contribution to χ. However, in many cases, it is not a very convincing explanation,[6] in particular because it would imply extremely narrow peaks. This description seems still less suited to our case as the temperature dependence of χ is still more pronounced whereas we expect a larger lifetime broadening of the charge carriers— considering the very short inelastic scattering time compatible with the behavior of the resistivity (see the Appendix). Conversely it is not easy to admit that a $Mo_{6n}Se_{6n+2}$ cluster carries a localized moment of $\approx 0.7\mu_B$. We are rather tempted to appeal to the Moriya-Kawabata description[7] of the effect of spin fluctuations in nearly ferromagnetic metals, which seems to be able to explain the Curie-Weiss-like temperature dependence of the susceptibility. However, another feature does not facilitate any comparison with the theoretical models: below about 20 K the susceptibility also becomes field dependent (see Fig. 3). This could be explained simply by supposing that the susceptibility contains a Curie contribution due to the presence of magnetic impurities: about 85 at. ppm of Fe^{3+} in $Cs_2Mo_{12}Se_{14}$ and 50 at. ppm in $Rb_4Mo_{18}Se_{20}$ would explain quite well the difference we observed between the low-field and high-field susceptibility. These estimations are consistent with the Fe concentrations which have been detected by atomic absorption photometry in powder samples coming from the same batches, i.e., 108 at. ppm and 57 at. ppm, respectively.

However, a consequence of this explanation is rather embarrassing because if we subtract such an impurity contribution from our data we are left with a corrected susceptibility which decreases below about 20 K (the dotted curve in Fig. 3). Manifestly a much more extensive study would be necessary to clarify the magnetic behavior of these compounds, including neutron diffraction and NMR experiments. Nevertheless, it already seems clear that charge carriers are rather localized and that correlation effects are unusually important in these superconductors.

III. THE SPECIFIC HEAT OF $Cs_2Mo_{12}Se_{14}$

The specific heat of a compressed powder sample of $Cs_2Mo_{12}Se_{14}$ has been measured between 0.3 and 10 K. The apparatus, including a He^3 cryostat, and the adiabatic technique employed have been described previously.[8]

In the normal phase the specific heat C_p can be analyzed, as usual, into a phonon βT^3 term plus a linear γT contribution. We obtain $\beta = 8.6$ mJ/mol K^4, which corresponds to a Debye temperature $\theta_D \approx 184$ K, according to the definition:

$$\beta = \frac{12}{5} r \mathcal{N} k_B \pi^4 \theta_D^{-3},$$

where r is the number of atoms per molecule, and $\mathcal{N}$ and

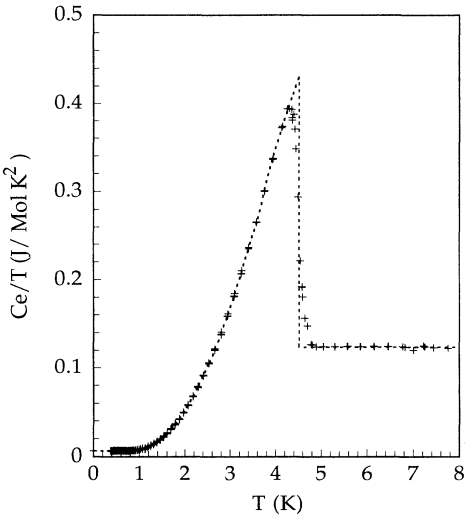

FIG. 4. Temperature dependence of the molar specific heat of $Cs_2Mo_{12}Se_{14}$ after subtraction of the lattice contribution. The broken curve shows the best-fitted mean-field transition (see text).

k_B are the Avogadro and Boltzmann constants, respectively. This compares fairly well with the phonon contribution observed in the CPS. The γ coefficient amounts to $\gamma = 124 \pm 8$ mJ/mol K^2; if it is interpreted as a Sommerfeld coefficient, i.e., as only due to the contribution of quasifree electrons, it corresponds to a density of states at the Fermi level $\mathcal{D}_{E_F} = 53$ states/eV molecule.

The superconducting transition is plotted in Fig. 4 after removal of the phonon term—which is not supposed to be modified by the transition. The dotted curve shows what would be the mean-field anomaly for a perfectly homogeneous sample having the same entropy and specific heat in the normal phase: the transition temperature of this "ideal" sample would be $T_c = 4.517$ K and its molar specific-heat jump ΔC would correspond to $\Delta C/\gamma T_c \approx 2.5$. This is an unusually large ratio, not only compared to the BCS value (1.43) but even compared to those usually observed in the CPS.[9] Even if we take for ΔC the difference between the highest and lowest measured value of C in the real sample on either side of the transition, we still find $\Delta C/\gamma T_c \approx 2.15$. Such an enhancement of this ratio is commonly considered as a strong-coupling effect.

To discuss this point a little further we need to compare the temperature dependence of the electronic specific heat C_{es} in the superconducting state with the theoretical predictions. As it appears in Fig. 5 our raw data largely depart from the BCS curve above about $T_c/T \approx 3$. This kind of behavior has been quite often observed in clean superconductors were it is attributed to a double (s-d) gap or to an anisotropic gap;[10] it is also observed in samples containing magnetic impurities.[11] As we shall show in the following, $Cs_2Mo_{12}Se_{14}$ has a fairly anisotropic Fermi surface and we have also some indications that this could involve several bands; however, it

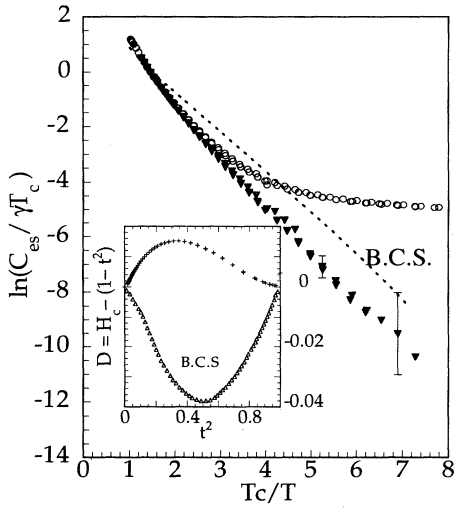

FIG. 5. Electronic specific heat of $Cs_2Mo_{12}Se_{14}$ in the superconducting state, expressed as $\ln(C_{es}/\gamma T_c)$ versus T_c/T. The triangles have been obtained by subtracting a $(\gamma_i T + b/T^2)$ term from the observed C_{es} (circles). The dashed line is that calculated from the BCS theory. In the inset is shown the deviation of the critical field from that of a simple parabolic law [the experimental points (crosses) are compared with the BCS prediction (triangles)].

seems quite unlikely that our powder sample could be considered as clean enough for the former interpretation to hold: on the contrary the data obtained on the single crystal and presented below clearly hint at a dirty-limit situation. We think that the anomalous behavior of C_{es} at low temperature is rather to be related to the latter interpretation, i.e., to the presence of magnetic impurities in our sample —as already suggested by the behavior of the susceptibility, in the preceding section. This interpretation is indirectly supported by the following consequence: it allows us to remove this contribution from the specific heat before calculating the thermodynamical critical field H_c: for instance, if we correct our data by linearly extrapolating the high-temperature behavior ($T_c/T < 3$) of the $\ln(C_{es})$ versus T_c/T curve down to the lowest temperatures we obtain $\mu_0 H_c(0) = 69.2$ mT and a characteristic parameter $\gamma T_c^2/H_c^2(0) = 0.133$. Conversely if we agree with the former interpretation we have to calculate $H_c(T)$ with the uncorrected data and we obtain $\mu_0 H_c(0) = 72.1$ mT; this yields a characteristic parameter $\mu_0 H_c(0) = 0.123$ which seems much too small, even for a strong-coupling superconductor.[12]

Our interpretation of the anomalous low-temperature specific heat cannot be checked easily, however, we remark that a similar behavior is observed in Zn and Mo, for concentrations of Mn and Fe, respectively, which are comparable to the Fe concentration in our sample. These impurities, which form well-defined magnetic moments, strongly alter the superconducting properties through the pair breaking effect of the *s-d* exchange interaction;[11] more precisely, the situation we are dealing with would correspond to the strong pair breaking limit which produces localized excited states within the superconducting (SC) gap near to the Fermi level.[13] This mechanism can lead to a specific heat contribution C_i which can be fitted to an equation of the form $C_i = \gamma_i T + b/T^n$ with $n \approx 2$–3 (Ref. 14)—where the second term has been interpreted as the high-temperature side of a Kondo anomaly. This analysis also seems to account for the low-temperature specific heat of our $Cs_2Mo_{12}Se_{14}$ sample, as shown in Fig. 5: supposing that the specific heat of the "pure" sample C_{es}^0 corresponds to the extrapolated high-temperature behavior—as described above—we deduce an extra contribution $C_i = C_{es} - C_{es}^0$ which can be fitted by taking $\gamma_i = 6.2$ mJ/mol K^2 and $b = 0.12$ mJ K/mol for $n = 2$.

Incidentally we think it would be worth examining thoroughly the origin of C_i because, if it is confirmed that $Cs_2Mo_{12}Se_{14}$ can give rise to a superconducting-Kondo system, other members of the large family built on the Mo_6X_8 cluster would certainly display the same behavior—and this could shed a new light on the formation of local moments in metals as well as on the electronic correlations in the CPS: issues which have been extensively discussed during the '60s and '70s but are still not completely clarified at present.

Let us now continue to compare our data with the BCS model or its strong-coupling extensions: first, following the assumptions made by Padamsee and co-workers[15] we can describe the corrected electronic specific heat shown in Fig. 5 by an α parameter [$\alpha = \Delta(0)/k_B T_c$] which is 2.175±0.05 —$\Delta(0)$ is the zero-temperature energy gap. According to Marsiglio and Carbotte[12] this value of α corresponds to a T_c/ω_{ln} ratio which is 0.112±0.008 —ω_{ln} is the mean phonon energy defined by Allen and Dynes;[16] this is in good agreement with what can be derived from $\Delta C/\gamma T_c \approx 2.5$ and it is also compatible with the value of the g parameter:

$$g = -\frac{1}{\gamma}\left(\frac{dC_{es}}{dT}\right)_{T_c}.$$

We obtain $g = -8.8 \pm 0.2$ which should be correlated with $T_c/\omega_{ln} = 0.096 \pm 0.005$ according to Marsiglio and Carbotte. Finally the parameter $\gamma T_c^2/H_c^2(0) \approx 0.133$ corresponds to $T_c/\omega_{ln} \approx 0.14$ but here our estimation as well as the proposed correlation are much less accurate. Therefore all these parameters are consistent with the strong coupling picture, which is also confirmed by the behavior of the characteristic function $D(t^2) \equiv H_c(t)/H_c(0) - (1 - t^2)$ plotted in the inset of Fig. 5. However, this agreement could be somewhat fortuitous: we showed in the preceding section that the magnetic susceptibility of $Cs_2Mo_{12}Se_{14}$ is indicative of strongly correlated charge carriers—this is borne out by the examination of the conductivity (see Sec. V)— and the Eliashberg model probably does not completely account for their coupling.

IV. CRITICAL-FIELD MEASUREMENTS

We studied the same $Cs_2Mo_{12}Se_{14}$ and $Rb_4Mo_{18}Se_{20}$ single crystals which were used in the resistivity

measurements[2,3] whose results are plotted in Fig. 2.

The volume of these samples is about 3.5×10^{-2} mm^3, which should correspond to a mass of ≈ 250 μg; they do not have a regular shape and show no well developed natural faces, however their longest dimension (≈ 0.7 mm) lies along the ternary axis and their transverse dimensions are of the order of 0.2–0.3 mm.

A. Upper critical field

The upper critical fields have been deduced by monitoring the resistive transitions induced by the magnetic field. The resistance measurements have been achieved by the usual four probe method with an ac bridge working at the frequency of 33 Hz. We used ultrasonically soldered indium contacts and checked that good ohmic behaviors were always obtained with the currents used (< 100 μA). The current was always applied in the c direction; however, due to the geometry of the samples and to the finite size of the current contacts, we expect a rather large dispersion ($\approx \pm5°$) of the direction of the current lines.

Our measurements were made in standard ^{4}He cryostats by sweeping the magnetic field produced by a Bitter coil of the Service National des Champs Intenses; the temperature being regulated within $\pm$ 0.05 K by using a capacitive detector. The sample was mounted on a rotating sample holder which allows an angular accuracy better than 1°. The low-field behavior has also been studied in a 0.7 T rotating electromagnet. We define the upper critical field H_{c_2} as the field which restores 90% of the normal resistance R_0; when magnetoresistance effects are significant we take the normal resistance at the intersection of the tangent at the middle of the transition with the extrapolation of the linear part of the high-field behavior. We have to point out that R_0 decreases linearly down to the lowest temperature we reached (1.3 K), with the same temperature coefficient[2] that is observed above T_c: $\frac{1}{R_0}\frac{dR_0}{dT} \approx 0.045$ K^{-1} and 0.115 K^{-1} for $Cs_2Mo_{12}Se_{14}$ and $Rb_4Mo_{18}Se_{20}$, respectively. In other words it seems that the resistivity would keep decreasing steadily and steeply, down to 1.3 K at least, if the superconducting transition had not taken place.

1. $Cs_2Mo_{12}Se_{14}$

We have plotted in Fig. 6 the resistive transitions observed at 4.05 K for different orientations of the field; the corresponding angular dependence of H_{c_2} is plotted in the inset and compared with what is given by the effective-mass model:[17]

$$H_{c_2}(\theta)^2 = \frac{H_{c_2}^{\|2}}{\cos^2\theta + \epsilon^2 \sin^2\theta} \quad (1)$$

with

$$\epsilon = \frac{H_{c_2}^{\|}}{H_{c_2}^{\perp}} = \left(\frac{m_\perp}{m_\|}\right)^{1/2}.$$

It is clear from this figure that our data are not well accounted for by this model, particularly near $\theta = 45°$. The lack of agreement is far beyond the inaccuracy of our measurements and is partly removed if we define H_{c_2} at 50% of the normal resistance, as the shape of the resistive transition changes with the direction of the field. The inhomogeneity of the sample is probably re-

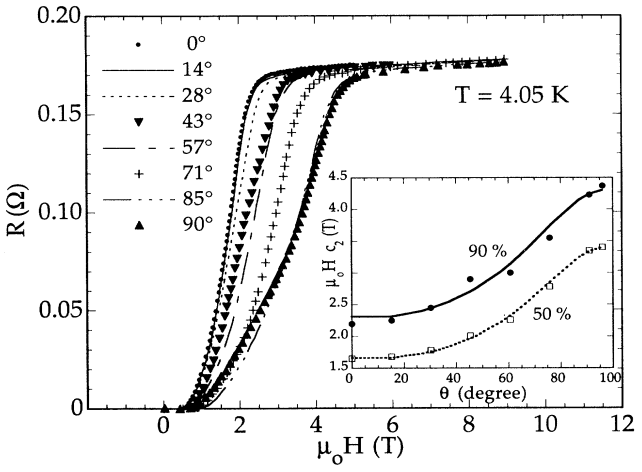

FIG. 6. The field induced resistive transitions of the $Cs_2Mo_{12}Se_{14}$ single crystal (current along c) for different orientations of the magnetic field with respect to the ternary axis at $T = 4.05$ K. In the inset is plotted the corresponding angular dependence of H_{c_2} which is defined at 90% (solid circles) or at 50% (squares) of the normal resistance; the curves are the best fits to the effective mass model [Eq. (1)].

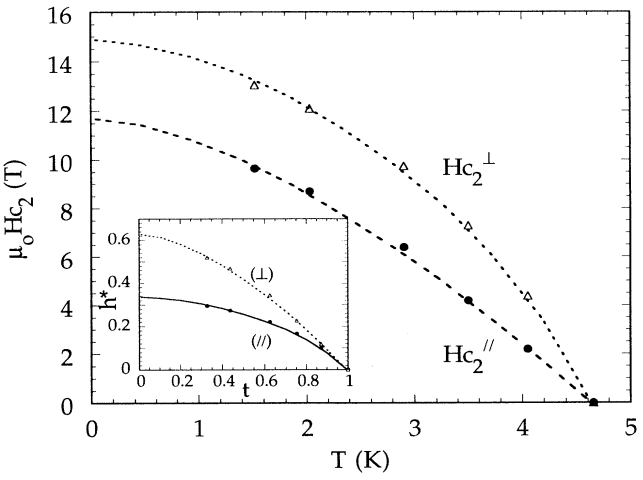

FIG. 7. The angular dependence of H_{c_2} (full dots: $H \parallel c$; open triangles: $H \perp c$). The curves are the best fits to Eq. (2), with $\alpha_\| = 2.1$, $\lambda_{so}^\| = 10$ and $\alpha_\perp = 5$, $\lambda_{so}^\perp = 2.5$, respectively. In the inset are plotted the reduced upper critical fields h^* as a function of $t = T/T_c$ [see text and Eq. (2)].

sponsible for this effect and for the rather large transition widths observed—especially in the low-field magnetic transitions, as we shall see in Sec. IV B. However, it is to be mentioned that this disagreement could also have a more fundamental origin: as we shall see below the paramagnetic limitation of H_{c_2} could disturb the nonlimited anisotropy.

From these data we deduce an anisotropy ratio at 4.05 K:

$$\left(\frac{H_{c_2}^{\perp}}{H_{c_2}^{\parallel}}\right)_{4.05\ \mathrm{K}} \approx 1.89.$$

The temperature dependence of H_{c_2} when the magnetic field is oriented parallel and perpendicular to the ternary axis is plotted in Fig. 7 and we shall compare it, now, with the theoretical model of Werthamer, Helfand and Hohenberg[18] (WHH). Taking into account the effect of the spin paramagnetism—characterized by the Maki parameter[19] α—and the counteracting effect of spin-orbit scattering—characterized by the relaxation time τ_{so} (which is supposed to be much greater than the spin-independent scattering time τ)—they derive, in the dirty limit, the well known implicit expression for the reduced critical field $\bar{h}$ [Eq. (29) in Ref. 18] :

$$\ln\left(\frac{1}{t}\right) = \left(\frac{1}{2}+\frac{i\lambda_{so}}{4\gamma}\right)\Psi\left(\frac{1}{2}+\frac{\bar{h}+\frac{1}{2}\lambda_{so}+i\gamma}{2t}\right)+\left(\frac{1}{2}-\frac{i\lambda_{so}}{4\gamma}\right)\Psi\left(\frac{1}{2}+\frac{\bar{h}+\frac{1}{2}\lambda_{so}-i\gamma}{2t}\right)-\Psi\left(\frac{1}{2}\right) \quad (2)$$

where Ψ is the digamma function and $\bar{h}$ is the reduced field defined by

$$\bar{h} = 2eH\frac{\langle v^2\rangle_{FS}\tau}{6\pi k_B T_c},$$

with

$$\gamma = \left[(\alpha\bar{h})^2 - \frac{1}{4}\lambda_{so}^2\right]^{1/2};\ \lambda_{so} = \frac{\hbar}{3\pi k_B T_c \tau_{so}};$$
$$t = \frac{T}{T_c} \quad \text{and} \quad \alpha = \frac{3\hbar}{2m\langle v^2\rangle_{FS}\tau}.$$

In this equation m is the free electron mass but $\langle v^2\rangle_{FS}$ corresponds to an average over the Fermi surface: in the isotropic case it is simply related to the effective mass by $\frac{1}{m^*} = \frac{1}{2E_F}\langle v^2\rangle_{FS}$; dealing with an uniaxial symmetry we have to replace these parameters by

$$\alpha_{\parallel} = \frac{\hbar}{2m\langle v_{\perp}^2\rangle_{FS}\tau} \quad \text{and} \quad \alpha_{\perp} = \frac{\hbar}{2m(\langle v_{\parallel}^2\rangle_{FS}\langle v_{\perp}^2\rangle_{FS})^{1/2}\tau}$$

for the parallel and perpendicular orientations, respectively, and therefore

$$\frac{\alpha_{\parallel}}{\alpha_{\perp}} = \left[\frac{\langle v_{\parallel}^2\rangle_{FS}}{\langle v_{\perp}^2\rangle_{FS}}\right]^{1/2} = \left[\frac{m_{\perp}}{m_{\parallel}}\right]^{1/2}.$$

We have compared our experimental data with this model by considering, as it is usual, the reduced field $h^* = \frac{\pi^2}{4}\bar{h}$ which is given by

$$h^* = \frac{H_{c_2}}{\left(\frac{-dH_{c_2}}{dt}\right)_{t=1}}.$$

The best fits are obtained with $\alpha_{\parallel} = 2.1 \pm 0.2$, $\lambda_{so}^{\parallel} = 10\pm2$ and $\alpha_{\perp} = 5\pm0.2$, $\lambda_{so}^{\perp} = 2.5\pm0.2$; they are displayed in the inset of Fig. 7. The corresponding initial slopes $-\mu_0(dH_{c_2}/dT)_{T_c}$ are respectively 4 T/K and 9.5 T/K.

From these values of α we can deduce what would be the upper critical fields $H_{c_2}^*(0)$ at $T = 0$, if there was no paramagnetic limitation: using $\alpha = \sqrt{2}H_{c_2}^*/H_{po}$ where H_{po} is the Chandrasekhar-Clogston field ($H_{po} = 1.84\ T_c$) we get

$$\mu_0 H_{c_2}^{\perp *}(0) = 30\ \mathrm{T} \quad \text{and} \quad \mu_0 H_{c_2}^{\parallel *}(0) = 12.7\ \mathrm{T}$$

which corresponds to an effective-mass ratio: $\frac{m_{\parallel}}{m_{\perp}} \approx 5.7$. This is significantly larger than the value (≈ 3.6) we have obtained from the angular dependence of H_{c_2} at 4.05 K. The difference comes from a less effective paramagnetic limitation in the parallel orientation and this is described, in the WHH model, by the larger value of the corresponding spin-orbit scattering parameter $\lambda_{so}^{\parallel}$. These results raise the problem of the origin of such high values of λ_{so}: a problem which is quite typical of the CPS (Ref. 20) and is directly related to their very large upper critical fields. Here we see that it should also include the question of the anisotropy of λ_{so}, upon which one finds very little information in the literature. One possible mechanism has been proposed by Andersen and co-workers:[21] they found that the calculated spin-orbit coupling is very sensitive to the local environment; this could lead, in nonperfect crystals, to a significant fluctuating potential. Although their bandstructure calculations indicated a nearly cubic symmetry of the Fermi surface, they expected strong anisotropy effects because the spin-orbit splitting is effective only in the [111] direction. Following this idea it is tempting to imagine that this kind of mechanism could also explain the deviation observed near $\theta = 45°$ in the angular dependence of H_{c_2} (Fig. 6). Finally we shall note that strong-coupling effects —which are not considered in the WHH model—could also modify the apparent λ_{so} and modify the anisotropy of H_{c_2} (Ref. 22). Another possible approach for the interpretation of these critical fields could be found in the valence-fluctuation mechanism proposed by Brandow:[1] as we shall show in the last section this model gives an attractive (qualitative) explanation of the main properties of the Chevrel-cluster-

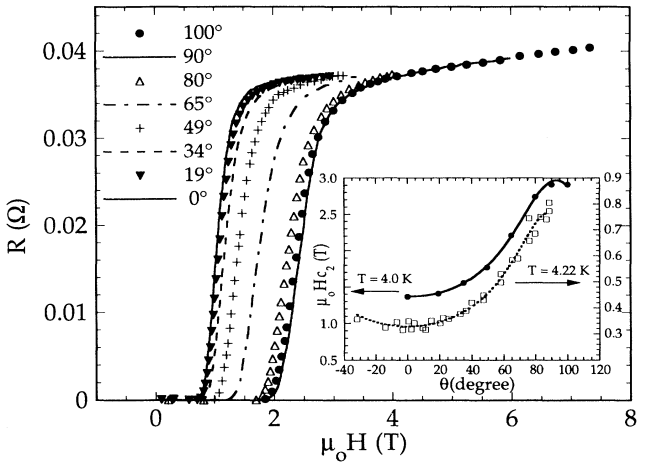

FIG. 8. The field induced resistive transitions of the $Rb_4Mo_{18}Se_{20}$ single crystal (current along c) for different orientations of the magnetic field at $T = 4.00$ K. In the inset is plotted the corresponding angular dependence of H_{c_2} (full dots, scale on the left) and also the data obtained at 4.22 K (crosses, scale on the right). H_{c_2} is defined at 90% of the normal resistance; the curves are the best fits to the effective mass model [Eq. (1)].

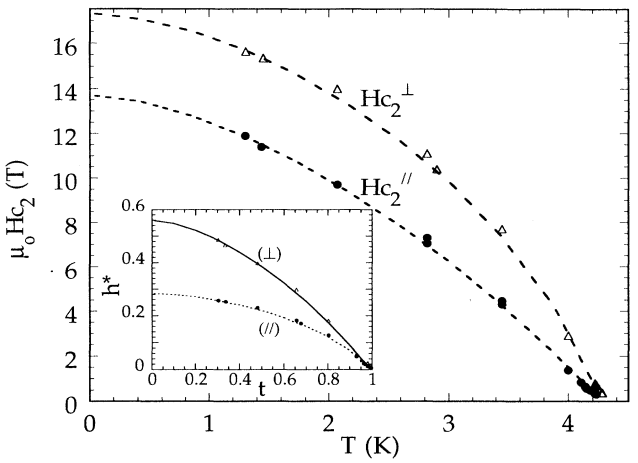

FIG. 9. The temperature dependence of H_{c_2} (full dots: $H \parallel c$; open triangles: $H \perp c$). The curves are the best fits to Eq. (2), with $\alpha_{\parallel} = 3$, $\lambda_{so}^{\parallel} = 7.5$ and $\alpha_{\perp} = 7.5$, $\lambda_{so}^{\perp} = 3.7$, respectively. In the inset are plotted the reduced upper critical fields h^* as a function of $t = T/T_c$ (see text).

based materials, and particularly of their very small coherence lengths which are expected to display unusual temperature dependences.

2. *$Rb_4Mo_{18}Se_{20}$*

As shown in Fig. 8 the field-induced resistive transitions have a smaller width and display a more regular angular dependence in $Rb_4Mo_{18}Se_{20}$ than in the previous compound. This indicates that we are dealing with a more homogeneous sample and will be confirmed by the low-field magnetization measurements (Sec. IV B). Consequently it has been possible to obtain significant results up to temperatures much nearer to T_c: for instance we show in the inset of Fig. 8 that the angular dependence of H_{c_2}—which is well described by the effective-mass model— is more pronounced at 4.22 K than at 4 K. This is due to an anisotropic paramagnetic limitation similar to the one described above for $Cs_2Mo_{12}Se_{14}$. Actually the effective-mass ratio we derive from the $H_{c_2}(\theta)$ curve at 4.22 K is $\frac{m_{\parallel}}{m_{\perp}} \approx 5.5$, in rather good agreement with what the WHH analysis gives us (see Fig. 9): $\alpha_{\parallel} = 3 \pm 0.2$, $\lambda_{so}^{\parallel} = 7.5 \pm 2$, and $\alpha_{\perp} = 7.5 \pm 0.5$, $\lambda_{so}^{\perp} = 3.7 \pm 0.5$.

The corresponding initial slopes $-\mu_0 \left(\frac{dH_{c_2}}{dT}\right)_{T_c}$ are respectively 5.7 T/K and 14.2 T/K, and from these values we deduce, as above, the nonlimited upper critical fields $H_{c_2}^*(0)$:

$$\mu_0 H_{c_2}^{\perp *}(0) \approx 42 \text{ T} \quad \text{and} \quad \mu_0 H_{c_2}^{\parallel *}(0) = 16.8 \text{ T}.$$

We also observe a linear transverse magnetoresistance which was already present in $Cs_2Mo_{12}Se_{14}$ but is here much more pronounced: $\frac{1}{R_0}\frac{dR}{dH} \approx 3.5 \times 10^{-2}$ T^{-1} and does not seem to depend on the temperature between 1.3 and 4 K.

B. Lower critical fields

The lower critical fields H_{c_1} have been determined with a low field SQUID magnetometer which is described elsewhere.[23] To cancel the spurious flux generated by the environment, a motor has been set up in the sample holder chamber to position the sample in one or the other coil of the astatic detection pair. The first flux penetration in the samples has been detected by monitoring the flux variation produced in the coils either by varying the temperature at constant field or by sweeping the field at constant temperature. The second method is more accurate and it has been improved by compensating the linear part of the signal coming from the pick-up coils. As the flux penetration is very progressive we determined H_{c_1} by fitting the first deviations from linearity to a $(H - H_{c_1})^2$ law, in accordance with the Bean model[24] (see inset in Fig. 10). Such a law is commonly observed, even in complex systems[25] where the Bean description seems to greatly oversimplify the mechanism of flux penetration, so we think that it could come from a kind of averaging effect and we should not take its physical significance too seriously. We shall rather consider that it provides a not too arbitrary definition of H_{c_1}.

To convert the external fields into internal fields we estimated the demagnetizing factors by likening each sample to the ellipsoid which surrounded it best. This usual approximation is particularly crude here because it supposes that the superconductivity is homogeneously dis-

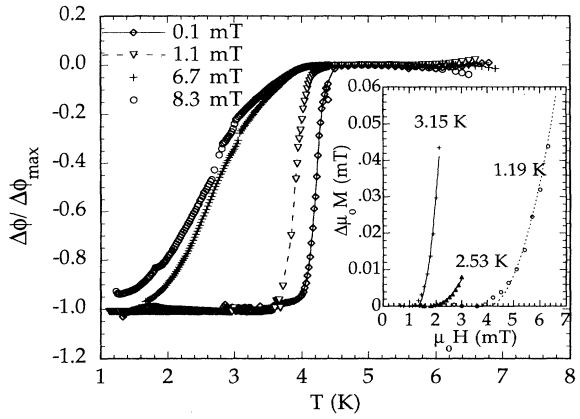

FIG. 10. The diamagnetic shielding of the $Cs_2Mo_{12}Se_{14}$ single crystal in different fields applied parallel to the c axis after zero-field cooling to 1.2 K. In the inset is plotted the initial nonlinear part of the magnetization at different temperatures (here the magnetization is plotted as a function of the *internal* field). The curves are the best $(H - H_{c_1})^2$ fits (see text).

tributed throughout the sample although only about 50% of it is in the Meissner state. Moreover, one should keep in mind that a supplementary demagnetization can occur in the regions of the sample where the surface is irregular; in our case, in view of the shape of these irregularities, we reckon this effect could be more important when the magnetic field is perpendicular to the ternary axis, and it could then contribute to an underestimate of $H_{c_1}^{\perp}$.

The low-field magnetic behavior of the $Cs_2Mo_{12}Se_{14}$ sample, which is exemplified in Fig. 10, is typical of an anisotropic extreme type-II superconductor. It also reveals that our crystal is not perfect: the diamagnetic shielding—i.e., the flux expulsion when the magnetic field is applied well below T_c—does not exceed about 50% and the magnetic transition is spread out on a temperature range of nearly 1–1.5 K, whereas the width of the resistive transition is only 0.3 K; moreover, the onset of the transition is near to 4.7 K in this case whereas the first noticeable magnetic expulsion does not occur before about 4.3 K. One should also notice in Fig. 10 that the vanishing of the diamagnetic shielding seems to be shifted quite rapidly to lower temperatures as the applied field is increased from 0 up to $\approx H_{c_1}$. Such a phenomenon is commonly attributed to chemical and/or structural inhomogeneities, leading to a distribution of all the parameters of the SC state throughout the sample. We had already observed its effects on the field induced recovery of the normal resistance (Sec. IV A 1), although the electrical conduction is much less sensitive to such an imperfection than the diamagnetic shielding. This different sensitivity is well illustrated in the present case where the resistance can vanish whereas about 50% of the sample remains normal.

The extreme type-II behavior of $Cs_2Mo_{12}Se_{14}$ is also associated, as usual, with strong pinning symptoms: the Meissner effect, for instance, amounts to less than 7% in fields lower than $H_{c_1}(0)$.

For the many reasons mentioned above, our estimate of H_{c_1} can only be rather crude in this compound and no meaningful temperature dependence can be deduced. Conversely, contenting ourselves with fitting our data to the BCS law, we obtain, at 0 K:

$$\mu_0 H_{c_1}^{\perp}(0) \approx 0.42 \pm 0.06 \text{ mT}$$
$$\text{and } \mu_0 H_{c_1}^{\parallel}(0) \approx 4.5 \pm 0.5 \text{ mT}.$$

The error ranges quoted here do not take into account our poor knowledge of the demagnetizing factors.

The low-field magnetic behavior of $Rb_4Mo_{18}Se_{20}$ is very similar to the one we observed in $Cs_2Mo_{12}Se_{14}$ but the crystal is of better quality: the diamagnetic expulsion is now complete, the transition is steeper and its onset corresponds fairly well to the beginning of the resistive transition. Flux pinning is also less effective and the Meissner effect amounts to about 40%. The values of H_{c_1} we determined between 3.2 K and 1.2 K can be approximately fitted to the BCS law and extrapolate to

$$\mu_0 H_{c_1}^{\perp}(0) \approx 0.14 \pm 0.02 \text{ mT}$$
$$\text{and } \mu_0 H_{c_1}^{\parallel}(0) \approx 0.2 \pm 0.025 \text{ mT at 0 K}.$$

V. THERMODYNAMICAL CRITICAL FIELD AND CHARACTERISTIC LENGTHS

In the high-κ limit the critical fields H_{c_1} and H_{c_2} are related by[26]

$$\left(\frac{H_{c_2}}{H_{c_1}}\right)^{1/2} = \frac{\sqrt{2}}{\kappa(\ln\kappa + 0.497)^{1/2}}, \tag{3}$$

where κ is the Ginzburg-Landau parameter. Within the effective mass model this equation can be extended to the anisotropic case[27] and gives for $Cs_2Mo_{12}Se_{14}$:

$$\kappa_{\parallel}(0) \approx 85 \pm 10 \text{ and } \kappa_{\perp}(0) \approx 490 \pm 50,$$

for $Rb_4Mo_{18}Se_{20}$:

$$\kappa_{\parallel}(0) \approx 530 \pm 60 \text{ and } \kappa_{\perp}(0) \approx 1080 \pm 130,$$

by using the zero-temperature values of the critical fields we estimated above. The thermodynamical critical fields can be derived from

$$H_c(0) = \frac{H_{c_2}^{*}(0)}{\sqrt{2}\kappa(0)} \tag{4}$$

which gives, by using the data coming either from the parallel or from the perpendicular orientation, respectively, for $Cs_2Mo_{12}Se_{14}$:

$$\mu_0 H_c(0) \approx 108 \pm 12 \text{ mT or } 53 \pm 6 \text{ mT},$$

for $Rb_4Mo_{18}Se_{20}$:

$$\mu_0 H_c(0) \approx 23 \pm 2.5 \text{ mT or } 25 \pm 3 \text{ mT}.$$

The agreement we obtain between the two determinations of $H_c(0)$ is quite good in $Rb_4Mo_{18}Se_{20}$ but rather poor in $Cs_2Mo_{12}Se_{14}$. This is probably related to the errors generated by the inhomogeneity of this crystal and by demagnetization effects, as discussed in Secs. IV A 1 and IV B: they have probably led us to underestimate $H_{c_1}^{\perp}$ and overestimate $H_{c_1}^{\parallel}$. Consequently we obtain also a κ ratio $\frac{\kappa_\perp}{\kappa_\parallel}$ which is about two times greater than the corresponding α ratio whereas the effective mass model identifies both of them with $\left(\frac{m_\parallel}{m_\perp}\right)^{1/2}$. The value of the thermodynamical field in $Cs_2Mo_{12}Se_{14}$ probably lies between our two estimates, and this agrees quite well with what has been determined from the specific heat measurements on the powdered sample ($\mu_0 H_c \approx 69.2$ mT; see Sec. III).

Conversely this good agreement makes us quite confident in the values of γ and $\mathcal{D}_{E_F}$ we can deduce for $Rb_4Mo_{18}Se_{20}$ from the H_c we determined above: taking $\mu_0 H_c = 24$ mT we obtain $\gamma \approx 23.7$ mJ/mol K^2 and $\mathcal{D}_{E_F} = 10$ states/eV molecule by taking the strong-coupling ratio $\gamma T_c^2/H_c^2(0) \approx 0.133$ which has been obtained for $Cs_2Mo_{12}Se_{14}$. A more probable value of this ratio could be 0.14 corresponding to $T_c/\omega_{\ln} = 0.11$; it yields to $\gamma \approx 25$ mJ/mol K^2, whereas the BCS ratio gives $\gamma \approx 30$ mJ/mol K^2.

The coherence lengths $\xi_\perp$ and $\xi_\parallel$ can be deduced from

$$H_{c_2}^{\parallel *}(0) = \frac{\phi_0}{2\pi\xi_\perp^2} \quad \text{and} \quad H_{c_2}^{\perp *}(0) = \frac{\phi_0}{2\pi\xi_\perp\xi_\parallel} \qquad (5)$$

—where ϕ_0 is the flux quantum $= 2 \times 10^{-15}$ Wb—and the penetration depths follow from $\lambda_\perp(0) = \kappa_\parallel(0)\xi_\perp(0)$ and $\lambda_\parallel(0) = \lambda_\perp(0)\frac{\xi_\perp(0)}{\xi_\parallel(0)}$.

For $Cs_2Mo_{12}Se_{14}$, we obtain

$$\xi_\perp(0) \approx 51 \text{ Å and } \xi_\parallel(0) \approx 21 \text{ Å};$$
$$\lambda_\perp(0) \approx 0.43\ \mu\text{m and } \lambda_\parallel(0) \approx 1\mu\text{m},$$

and for $Rb_4Mo_{18}Se_{20}$

$$\xi_\perp(0) \approx 43 \text{ Å and } \xi_\parallel(0) \approx 17 \text{ Å};$$
$$\lambda_\perp(0) \approx 2.3\ \mu\text{m and } \lambda_\parallel(0) = 5.4\ \mu\text{m}.$$

VI. DISCUSSION

We shall now compare these results to those obtained in the CPS. Despite the great amount of work which has been done on these compounds only a few results are available upon the thermodynamical properties, penetration lengths, and anisotropy of the superconducting state. We summarized these results in Table I. A first look at these data shows that the coherence lengths of the finite chain compounds $Cs_2Mo_{12}Se_{14}$ and $Rb_4Mo_{18}Se_{20}$ are comparable to the smallest observed in the CPS.

Another striking result emerging from Table I is that we find in the finite-chain compounds the same kind of anisotropy as in the CPS, but more pronounced. Its origin in the latter is far from being understood,[28] whereas in the former a plausible explanation could be provided by the band structure.

TABLE I. Comparison between the characteristic parameters of the superconducting phase in the Mo_6X_8-cluster-based compounds.

Compound	T_c (K)	$\lambda(0)$ (μm)	$\xi(0)$ (Å)	ϵ^{2c}	$\mu_0 H_c(0)$ (μT)	γ (mJ/cm^3 K^2)
$PbMo_6S_8$	12.6[b]	(0.37)[e]	25[b]		(242.5)[e]	0.63[b]
	12		$\xi_\parallel = 22; \xi_\perp = 26$	0.71		
	14.4[a]	0.24[a]			219.5[a]	0.58[a]
$SnMo_6S_8$	11.8[b]	(0.3)[e]	29[b]		(200)[e]	0.48[b]
	13.8[a]	0.24[a]				0.46[a]
$LaMo_6Se_8$	10.8[b]	(0.55)[e]	24[b]		(170)[e]	0.42[b]
	11[a]	0.4[a]				
$SnMo_6Se_8$	6.8		$\xi_\parallel = 34; \xi_\perp = 40$	0.71		
$SnMo_6S_1Se_7$	3.8[a]	1.09[a]				
$PbMo_6Se_8$	3.8[b]	(0.85)[e]	74[b]		(30)[e]	0.15[b]
	6.75			0.67		
$Cs_2Mo_{12}Se_{14}$	4.5	$\lambda_\parallel = 1; \lambda_\perp = 0.43$	$\xi_\parallel = 21; \xi_\perp = 51$	0.18	69.2	0.315
$Rb_4Mo_{18}Se_{20}$	4.4	$\lambda_\parallel = 5.4; \lambda_\perp = 2.3$	$\xi_\parallel = 17; \xi_\perp = 43$	0.16	(24)[d]	(0.04)[d]
Tl_2Mo_6Se[f]	6.5	$\lambda_\parallel = 2.7; \lambda_\perp = 35$	$\xi_\parallel = 325; \xi_\perp = 25$	170	(1.9)[d]	< 0.005

[a]From P. Birrer and co-workers (see Ref. 41).
[b]From Ø. Fischer, Ref. 20.
[c]The values of ϵ^2 are deduced from the ratio of $(dH_{c_2}/dT)_{T_c}$ in the parallel and perpendicular directions [see Eq. (1)] except for $PbMo_6Se_8$ where it comes from the comparison of the values of H_{c_2} at 4.2 K.
[d]H_c is obtained by applying Eqs. (3) and (4) to our values of H_{c_2} and H_{c_1}; γ is deduced by using the same strong-coupling parameter we derived for $Cs_2Mo_{12}Se_{14}$ (see Sec. V).
[e]These values are deduced from the other data (T_c, γ, and ξ) by applying the BCS formula.
[f]See Ref. 23. The other data upon the CPS come from Ref. 30.

A. Band structure

No band-structure calculations have been done on the finite-chain compounds, however, the electronic structures of the $Mo_{3n}Se_{3n+2}$ clusters ($2 \leq n \leq 6$) have been analyzed.[32] One of the main results coming out of this work is the close analogy between the highest occupied molecular orbital (MO) in the even-n clusters: they are bonding orbitals, primarily of Mo d character and $(x^2 - y^2)$ symmetry, so they are expected to be negligibly perturbed upon the formation of intercluster Mo-X bonds. This should lead to rather localized levels and a high density of states at the Fermi level. As the length of the clusters increases (n = 4,6,...) these MO remain quite localized upon the terminal Mo atoms and it is anticipated that the electronic coupling between the ends of the clusters could be very weak. Considering the poor overlap of these δ-type orbitals with the atomic orbitals centered upon the capping chalcogens, Hughbanks and Hoffmann suggested that the electronic properties of these materials could be mostly determined by the intercluster Mo-Mo overlap, even though their structural characteristics are determined by Mo-X intercluster bonding. Our results concerning the anisotropy of $Cs_2Mo_{12}Se_{14}$ and $Rb_4Mo_{18}Se_{20}$ agree with this picture in which the intercluster electron transfer *via* the ends of the clusters (perpendicular to the c axis) would be easier than the intracluster transfer (along the c axis). Table I gives another indication that these "δ" frontier orbitals form a great part of the conduction band: $\mathcal{D}_{E_F}$ seems to decrease when n increases, which is compatible with the reduction of the number of these states as the length of the clusters increases.

Within the same framework we expect that the lengthening of the clusters up to the formation of infinite chains $(Mo_3Se_3)_\infty$ will progressively lead to the disappearance of the "δ" orbitals; at the Fermi level the place will be left for a broad a_2 band composed of d_{xz} orbitals winding along the c axis (the "helix" band in Ref. 29). Such a quasi-one-dimensional band structure with a low density of states at E_F is consistent with the behavior of $Tl_2Mo_6Se_6$ (Ref. 33) which is also summarized in Table I.

B. Electronic conduction

Before discussing the electron transport in $Cs_2Mo_{12}Se_{14}$ and $Rb_4Mo_{18}Se_{20}$ we shall recall what is the present state of our knowledge about the parent compounds.

As mentioned above, few measurements have been done on CPS single crystals, moreover, the available results have not always been obtained on single phase samples. We shall pay special attention to $PbMo_6S_8$ which has been the most extensively studied and shows no sign of a low-temperature phase transition. Its resistivity is estimated typically between 100 and 1000 $\mu\Omega$ cm at 300 K, and it decreases continuously with temperature down to T_c, leading to ρ_{300}/ρ_{T_c} of the order of 10. Such a large resistivity has been assigned principally to a very short mean-free path ℓ either by arguing[34] that its tendency to saturate at room temperature was due to ℓ approaching the size of the clusters ($\sim$ 6 Å) or by using a simple effective-mass model[20] with a spherical Fermi surface and a carrier concentration (n) corresponding to 1–2 electrons per cluster. The corresponding order of magnitude for the effective mass (m^*) and Fermi energy (E_F) would be 5–10 m_e and 0.2–0.5 eV, respectively, which is consistent with a density of states at the Fermi level $\mathcal{D}_{E_F} \approx$ 10–20 states/eV molecule and with a London penetration depth $\lambda_L \approx 0.5$ μm (see Table I). The Fermi velocity would be $v_F \approx 1.5\times10^7$ cm/s and the electron scattering time $\tau \approx 1 - 2 \times 10^{-14}$ s just above T_c, yielding a $\ell \approx$ 20–30 Å and a coherence length $\xi_0 = \frac{\hbar v_F}{\pi\Delta} \approx$ 150–200 Å. The corresponding dirty limit coherence length $\xi(0) = (\xi_0 \ell)^{1/2}$ would be a little too high ($\approx$ 50–75 Å) but this could be ascribed to the inaccuracy of the data and particularly to our poor knowledge of the conductivity of these compounds. For the same reason the electron-phonon interaction parameter λ can be only crudely estimated: taking $\lambda \approx 1$ (Ref. 35) would imply a temperature dependence of the resistivity amounting to ≈ 2.5 $\mu\Omega$ cm/K above $\sim \theta_D/2 \approx$ 100–200 K (Ref. 36) and a phonon-limited scattering time $\tau_{ph} \approx 0.5\times10^{-14}$ s at 200 K;[37] these values would be compatible with the signs of saturation of the resistivity sometimes observed at room temperature.

This description of the CPS looks quite coherent but it leaves aside a lot of badly understood features, principally the following.

(a) It leads to a tiny value of the phonon-limited mean-free path $\ell_{ph} = v_F \tau_{ph} \approx 10$ Å at 200–300 K, which is incompatible with conventional electron-phonon theory and with the value of λ which can be derived phenomenologically.[38]

(b) The fact that T_c seems to "peak when the resistivity is as bad as it can be and still be metallic," (Ref. 38).

(c) The fact that such narrow bands can give rise to superconductivity instead of destabilizing into some insulating phase.[39]

(d) Moreover, the small $\xi(0)$ cannot be explained only by the low v_F resulting from these flat bands; a very small mean-free path $\ell \leq 20$ Å must also be invoked which seems difficult to attribute to chemical or structural defects, especially since it is almost independent of the compound considered and of its preparation.

Such features are far from being exclusive to the CPS, they are reminiscent of the superconducting cuprates in particular, and more generally of those superconductors which Uemura and co-workers have labeled as "exotic" (Ref. 40)—among which, a decade ago, Anderson and Yu[39] had already recognized "bad actors"—and in which operates, according to Brandow[1] the same valence-fluctuation scenario.

Within this wider and wider family of superconductors the chain compounds of general formula $M_{2n-2}Mo_{6n}Se_{6n+2}$ seem to occupy an extreme position and therefore could give us very valuable information.

Considering successively the features (a)–(d) above we notice first that the thermal component of the re-

sistivity of $Cs_2Mo_{12}Se_{14}$ and $Rb_4Mo_{18}Se_{20}$ along the chains exceeds 5 mΩ cm at 300 K; moreover, it displays pronounced signs of high-temperature saturation —especially in the former compound where a nonmetallic behavior is observed above $\approx$ 100 K (see Fig. 2). The very low conductivity of these materials is correlated with large penetration depths λ_L (see Table I), i.e., with small n/m^* ratios. As we show in the Appendix, applying a quasi-free-electron description to these compounds leads to values of the Fermi energy and velocity which are still smaller than in the CPS.

Finally we shall not forget that they both display, in the normal state, a magnetoresistance with a linear field dependence and a conductivity which keeps increasing down to 1.5–1.3 K at least. Therefore, in many respects, the condensation of the Mo_6Se_8 clusters into finite chains still enhances the unusual character of the electron system.

We notice also that the coherence lengths $\xi(0)$ are very similar in all these compounds and always of the same order of magnitude as the size of the clusters or chains, when we are dealing with *finite* chains, whereas $\xi_{\|}(0)$ is an order of magnitude larger in the infinite-chain compound $Tl_2Mo_6Se_6$. We think this comparison strongly hints at a reduction of the coherence length not principally due to defects in the former compounds, but rather due to the localization of the carriers within the clusters or chains. The localized character of the wave functions on which is built the superconducting state has already been recognized as taking a major part in the unusual properties of the CPS, particularly in their very high H_{c_2}. Our feeling is that the pairing of carriers in the SC state could also have some local (non-BCS) character.

C. T_c systematics

Uemura and co-workers[40] have claimed that the transition temperature could be correlated with $1/\lambda^2 \propto n_s/m^*$ in the CPS as well as in the high T_c's and other "exotic" superconductors. According to them the same linear relationship describes the initial increase of T_c with $1/\lambda^2$ in each family of compounds. For higher values of $1/\lambda^2$ T_c tends to a saturation and even decreases. In the case of the CPS we find only a couple of data points on their universal straight line, and the whole set of data can be interpreted quite differently: Birrer and co-workers[41] for instance recognize a power-law dependence which comes close to $T_c \propto (1/\lambda)^{2/3}$. The results we obtained upon the finite chain compounds do not reinforce these correlations.

Our results show that $Cs_2Mo_{12}Se_{14}$, $Rb_4Mo_{18}Se_{20}$ and —*a fortiori*—$Tl_2Mo_6Se_6$ cannot be related to the CPS by either kind of law. This is a clear indication that anisotropy is one of the features which prevent T_c from being closely correlated with simple parameters.

VII. CONCLUSION

Although this is not revealed by a simple correlation law, $Cs_2Mo_{12}Se_{14}$ and $Rb_4Mo_{18}Se_{20}$ are certainly to be classified among the "exotic" superconductors, according to the criteria proposed by Uemura and co-workers: they have short coherence lengths ξ, large T_c/T_F ratios,[42] and strongly enhanced low-temperature susceptibilities indicating strongly correlated carriers. They are also remarkable for their macroscopic penetration depths and for their high normal-state resistivities which display a large nonphononic temperature dependence down to 1.5 K at least.

Some of these features have been noticed quite early in various compounds—the low conductivity of the $A15$'s and the short coherence length of the CPS, for instance—and it has been suggested[38,39] that they could be related to a common mechanism. Recently, Brandow[1] has proposed a theoretical model which assigns the common origin of these "exotic" behaviors to a valence-fluctuation mechanism—operating together with the phonons. The starting point of this model is a normal Fermi-liquid state having strong electronic correlations of the type encountered in valence-fluctuation and heavy-fermion materials. An Anderson lattice form of model Hamiltonian is used in which the Hubbard U interaction can be assigned to a *cluster* of atoms rather than to a single ion; another important ingredient is a "conduction band" which has substantial hybridization with the "localized" or strong-U orbitals. In the CPS, and in the Chevrel-cluster-based compounds we studied, it is quite plausible that such a conduction band could result from some of the p orbitals of the chalcogenide ions—providing hybridizing bridges between the clusters. Within this framework we could interpret the low T_c of these compounds as being due to a low charge-transfer energy Δ_{CT} (the energy difference between the localized level and the centroid of the conduction band) which induces too repulsive a pair interaction $V_{kk'}$ and brings the system to the threshold of a magnetic instability. A significant reduction of T_c could also result from pair-breaking effects due to short quasiparticle lifetime caused by strong quasiparticle scattering.

The valence-fluctuation scenario of Brandow seems very attractive and, adopting the same point of view, it is tempting to draw a parallel between the apical oxygens in the cuprates and the capping seleniums in $M_{2n-2}Mo_{6n}Se_{6n+2}$—at the ends of the extended clusters—which could explain the higher T_c/γ ratio in $Rb_4Mo_{18}Se_{20}$.

Even leaving apart such a promising prospect, this work has convinced us that the Mo_6X_8 blocks could still be used to build very interesting systems and that their study could help in puzzling out some of the issues raised by the "exotic" superconductivity.

APPENDIX

We start with the London penetration depth $\lambda_L = \left(\frac{m^*c^2}{4\pi ne^2}\right)^{1/2}$ and its dirty-limit and anisotropic modification

$$\lambda_{\|} = 0.615\lambda_L^{\|}\left(\frac{0.18\hbar}{k_B T_c \tau}\right)^{1/2},$$

which is usually quoted by replacing the fraction by ξ_0/ℓ in isotropic systems.

Taking $\tau = 10^{-14}$ s yields $\lambda_{\|}(0) \approx 3.35\,\lambda_L^{\|}(0)$ and $\frac{n}{\beta_{\|}} = 3\times10^{20}$ cm^{-3} in the case of $Cs_2Mo_{12}Se_{14}$ (β is the ratio of the effective mass m^* to the free electron mass).

In order to get a not too small density of states $\mathcal{D}_{E_F}$, we choose $\beta_{\|} \approx 10$ and $\beta_{\perp} \approx 2$ which corresponds to $n \approx 3\times10^{21}$ cm^{-3} (i.e., about two carriers per formula unit) and to $\mathcal{D}_{E_F} \approx 13.6$ states/eV molecule; this value is still too small, compared with our measurements, however, it already leads to a very small Fermi energy $E_F \approx 0.23$ eV and velocity $v_F^{\|} \approx 9\times10^6$ cm/s. Accordingly the mean-free path ℓ_i would be only 9 Å.

Surprisingly these unusual values of $\beta_{\|}$ and τ yield a fairly realistic residual resistivity $\rho(0) \approx 1$ mΩ cm and coherence length $\xi^{\|}(0) = (\xi_0^{\|}\ell_i)^{1/2} \approx 50$ Å.

The phonon-limited mean-free path $\ell_{\rm ph}$ we can estimate within the same framework is also puzzling: following Allen[37] we estimate $\tau_{\rm ph}$ for $T \geq \theta_D/2$, using

$$\frac{\hbar}{\tau_{\rm ph}} \approx 2\pi\lambda k_B T.$$

Taking $\lambda \approx 1$ we find $\tau_{\rm ph} \approx 1.2\times10^{-14}$ s and $\ell_{\rm ph} \approx 11$ Å at 100 K. Such a small value is difficult to understand, however, it gives a phonon contribution to the resistivity which is still too small (≈ 1 mΩ cm) to account for the measured increase of the resistivity between T_c and 100 K (≈ 5 mΩ cm).

With a larger $\tau = 10^{-13}$ s we obtain by the same way $\frac{n}{\beta_{\|}} = 2.8\times10^{19}$ cm^{-3}, $\mathcal{D}_{E_F} = 6$ states/eV molecule, $E_F \approx 0.05$ eV, and $v_F^{\|} \approx 4\times10^6$ cm/s; ℓ_i is then 40 Å, $\rho(0)$ and $\xi^{\|}(0)$ are only slightly larger than above, but the phonon contribution to the resistivity is reduced to 150 μΩ cm at 100 K. To obtain a density of states in agreement with our specific-heat measurements ($\mathcal{D}_{E_F} \approx 53$ states/eV molecule) we need to take $\beta_{\|} \approx 50$ and $\beta_{\perp} \approx 10$, which leads to $E_F \approx 0.026$ eV.

Finally we apply the same treatment to $Rb_4Mo_{18}Se_{20}$. With $\tau = 10^{-14}$ s, $\beta_{\|} \approx 10$, and $\beta_{\perp} \approx 2$ we deduce $n \approx 10^{20}$ cm^{-3}, $\mathcal{D}_{E_F} = 6.6$ states/eV molecule, $E_F \approx 0.024$ eV, and $v_F^{\|} \approx 2.9\times10^6$ cm/s. This yields $\ell_i \approx 3$ Å and $\rho(0) \approx 33$ mΩ cm, which is not very satisfactory. Taking $\tau = 10^{-13}$ s leads to a larger $\ell_i \approx 13$ Å but $\mathcal{D}_{E_F}$ is reduced and E_F is then much too small (≈ 0.005 eV).

Our feeling is that applying the quasi-free-electron model to the CPS already leads to a not very convincing picture, but when applied to the finite-chain compounds this model gives still worse results: it cannot conciliate the small concentration of carriers with the rather large density of states $\mathcal{D}_{E_F}$ without implying unphysical mean-free paths. Conversely we think that the contradictions observed in these compounds point out particular electron correlations which also operate, but more discretely, in the CPS.

[1] B.H. Brandow, Int. J. Mod. Phys. B **8**, 3859 (1994).

[2] P. Gougeon, M. Potel, J. Padiou, and M. Sergent, Mater. Res. Bull. **22**, 1087 (1987).

[3] P. Gougeon, M. Potel, J. Padiou, and M. Sergent, Mater. Res. Bull. **23**, 453 (1988).

[4] The value of the resistivity of $Cs_2Mo_{12}Se_{14}$ published in Ref. 2 was in error by a factor 10.

[5] F.S. Delk and M.J. Sienko, Inorg. Chem. **19**, 1352 (1980); D.C. Johnston and R.N. Shelton, J. Low Temp. Phys. **26**, 561 (1977); N.E. Alekseevskii, V.I. Nizhankowskii, J. Beille, and E. du Tremolet de Lachesserie, *ibid.* **72**, 241 (1988).

[6] J.M. Tarascon, F.J. DiSalvo, D.W. Murphy, G. Hull, and J.V. Waszczak, Phys. Rev. B **29**, 172 (1984).

[7] T. Moriya and A. Kawabata, J. Phys. Soc. Jpn. **34**, 639 (1973).

[8] A. Junod, E. Bonjour, R. Calemczuck, J.Y. Henry, J. Muller, G. Triscone, and J.C. Vallier, Physica C **211**, 304 (1993).

[9] See, for instance, F. Pobell, D. Rainer, and H. Wühl, in *Superconductivity in Ternary Compounds I*, edited by M.B. Maple and Ø. Fischer, Topics in Current Physics Vol. 32 (Springer-Verlag, Berlin, 1982), p. 251; S. Morohashi, K. Noto, N. Kobayashi, and Y. Muto, Physica B **108**, 929 (1981).

[10] See, for instance, G. Gladstone, M.A. Jensen, and J.R. Schrieffer, in *Superconductivity*, edited by R.D. Parks (Marcel Dekker Inc., New York, 1969), Vol. 2, p. 665, and references therein.

[11] For a review see, for instance, S. Takayanagi and T. Sugawara, J. Phys. Soc. Jpn. **38**, 718 (1975) and references therein; M.B. Maple, in *Magnetism*, edited by H. Suhl (Academic Press, New York, 1973), Vol. V, p. 289.

[12] F. Marsiglio and J.P. Carbotte, Phys. Rev. B **33**, 6141 (1986).

[13] H. Shiba, Prog. Theor. Phys. **50**, 50 (1973); M. Fowler and K. Maki, Phys. Rev. B **1**, 181 (1970).

[14] H.V. Culbert and A.S. Edelstein, Solid State Commun. **8**, 445 (1970); C.A. Luengo, M.B. Maple, and W.A. Fertig, *ibid.* **11**, 1445 (1973).

[15] H. Padamsee, J.E. Neighbor, and C.A. Shiffman, J. Low Temp. Phys. **12**, 387 (1973).

[16] P.B. Allen and R.C. Dynes, Phys. Rev. B **12**, 905 (1975).

[17] C. Caroli, P.G. De Gennes, and J. Matricon, Phys. Kondens. Mater. **1**, 176 (1963); L.P. Gor'kov and T.K. Melik-Barkhudarov, Sov. Phys. JETP **18**, 1031 (1964); this is reviewed, for instance, by N.R. Werthamer, in *Superconductivity* (Ref. 10), Vol. 1, p. 361 and by H. Teichler, in *Anisotropy Effects in Superconductors*, edited by H.W. Weber (Plenum Press, New York, 1976), p. 7.

[18] N.R. Werthamer, E. Helfand, and P.C. Hohenberg, Phys. Rev. **147**, 295 (1966).

[19] K. Maki, Phys. Rev. **148**, 362 (1966).

[20] See, for instance, Ø. Fischer, Appl. Phys. **16**, 1 (1978).

[21] O.K. Andersen, W. Klose, and H. Nohl, Phys. Rev. B **17**, 1209 (1978).

[22] E. Schachinger, H.G. Zarate, M. Schossmann, and J.P. Car-

botte, J. Low Temp. Phys. **63**, 1 (1986).
[23] R. Brusetti, P. Monceau, M. Potel, P. Gougeon, and M. Sergent, Solid State Commun. **66**, 181 (1988).
[24] C.P. Bean, Phys. Rev. Lett. **8**, 250 (1962).
[25] J.C. Martinez, J.J. Préjean, J. Karpinski, E. Kaldis, and P. Bordet, Solid State Commun. **75**, 315 (1990).
[26] R.A. Klemm and J.R. Clem, Phys. Rev. B **21**, 1868 (1980).
[27] See, for instance, R.A. Klemm, in *Electronic Properties of Inorganic Quasi-One-Dimensional Materials*, edited by P. Monceau (D. Reidel Publishing Company, Dordrecht, 1985), Vol. 1, p. 195 and Ref. 23.
[28] According to Nohl and co-workers (Ref. 29) it is the hybridization between the t_{1u} and e_g bands which produces a noncubic distortion of the Fermi surface in the ternary CPS but not in the binaries. Actually these two kinds of compounds display different behaviors in that respect, but Mo_6Se_8 does not seem to be isotropic either: critical-field measurements indicate that the effective mass is approximately 25% lower along the ternary axis (Ref. 30). Several parasitic effects—including oxygen pollution and low-temperature distortions (Ref. 31)—could complicate the real state of these compounds.
[29] H. Nohl, W. Klose, and O.K. Andersen, in *Superconductivity in Ternary Compounds I* (Ref. 9), p. 165.
[30] M. Decroux and Ø. Fischer, *Superconductivity in Ternary Compounds II* (Ref. 9), p. 57.
[31] J.C. Phillips, J.M. Vandenberg, and K.M. Rabe, Europhys. Lett. **18**, 349 (1992); R. Flükiger and R. Baillif, in *Superconductivity in Ternary Compounds I* (Ref. 9), p. 113; J.D. Jorgensen, D.G. Hinks, and G.P. Felcher, Phys. Rev. B **35**, 5365 (1987).
[32] T. Hughbanks and R. Hoffmann, J. Am. Chem. Soc. **105**, 1150 (1983); A. Le Beuze, P. Lamandé, R. Lissilour, and H. Chermette, Phys. Rev. B **31**, 5094 (1985).
[33] R. Brusetti, A. Briggs, O. Laborde, M. Potel, and P. Gougeon, Phys. Rev. B **49**, 8931 (1994) and Ref. 9.
[34] J.A. Woollam and S.A. Alterovitz, Phys. Rev. B **19**, 749 (1979).
[35] See Ref. 20. The value of λ is also commonly estimated by comparing the electronic specific-heat coefficient γ with the Pauli contribution to the susceptibility; however, such a derivation is far from being easy in the CPS because the measured susceptibility is often temperature dependent and anisotropic (Refs. 5, 6).
[36] S.D. Bader, S.K. Sinha, B.P. Schweiss, and B. Renker, in *Superconductivity in Ternary Compounds I* (Ref. 9), p. 223.
[37] P.B. Allen, Comments Cond. Mat. Phys. **15**, 327 (1992); see also the Appendix.
[38] P.W. Anderson and C.C. Yu, in *Highlights of Condensed-Matter Theory*, Proceedings of the International School of Physics "Enrico Fermi," Course 89, edited by F. Bassani *et al.* (North-Holland, Italy, 1985), p. 767.
[39] P.W. Anderson, in *Ternary Superconductors*, edited by G.K. Shenoy *et al.* (Elsevier, North-Holland, 1981), p. 309.
[40] Y.J. Uemura, L.P. Le, G.M. Luke, B.J. Strenlieb, W.D. Wu, J.H. Brewer, T.M. Rieseman, C.L. Seaman, M.P. Maple, M. Ishikawa, D.G. Hinks, J.D. Jorgensen, G. Saito, and H. Yamochi, Phys. Rev. Lett. **66**, 2665 (1991).
[41] P. Birrer, F.N. Gigax, B. Hitti, E. Lippelt, A. Schenck, M. Weber, D. Cattani, J. Cors, M. Decroux, and Ø. Fischer, Phys. Rev. B **48**, 16 589 (1993).
[42] The Fermi temperature T_F which can be deduced from the penetration depths λ and Sommerfeld constant γ, according to the procedure proposed by Uemura and co-workers, is $T_F \approx 300$ K for $Cs_2Mo_{12}Se_{14}$ (see the Appendix).